Flexural behavior of precast concrete box beams post-tensioned with unbonded, carbon-fiber-composite cables

Nabil Grace, Tsuyoshi Enomoto, Ahmed Abdel-Mohti, Yahia Tokal, and Sreejith Puravankara

Editor's quick points

- This paper offers a solution to the corrosion of steel reinforcement in prestressed concrete box-beam bridges due to seepage of moisture and chemicals through longitudinal cracks in the deck slab between adjacent beams.
- Replacing conventional steel reinforcement with non-corroding, fiber-reinforced polymer reinforcement is one way to eliminate corrosion.
- The effect of unbonded, longitudinal post-tensioning of carbon-fiber-composite cables on the flexural behavior of the bridge models is investigated.

Corrosion of steel reinforcement, resulting from aggressive environmental conditions and the use of deicing salts, is one of the major causes for deterioration of concrete structures. A potential solution is to use fiber-reinforced polymer (FRP) reinforcement.

This paper presents the flexural behavior of precast concrete box-beam bridge systems that are prestressed and reinforced with carbon-fiber-composite cables (CFCC). Three box-beam bridge models were designed, constructed, instrumented, and tested to failure. The three bridge models were of the same cross section and dimensions and were reinforced with the same amount of bonded, bottom pretensioned; bonded, bottom nonprestressed; and bonded, top nonprestressed strands. This investigation mainly presents the effect of unbonded, longitudinal post-tensioning of CFCC on the flexural behavior of the bridge models.

To test the effect of unbonded, longitudinal post-tensioning of CFCC on flexural behavior, one specimen contained unbonded, longitudinal post-tensioned CFCC strands, the second specimen contained unbonded, longi-

tudinal CFCC strands with zero post-tensioning force, and the third specimen did not contain unbonded, longitudinal CFCC strands.

Background

Figures 1 and **2** are examples of corrosive deterioration of concrete structures.[1] Exposed structures such as highway bridges are more vulnerable to environmental deterioration. According to the National Bridge Inventory database,[2] there are 614,083 bridges in the United States, of which 87,801 are classified as structurally deficient and 79,860 are classified as functionally obsolete.

ceed concrete box beams are commonly used for bridge construction. Some of their typical advantages[3] are

- great torsional stiffness, making box-beam sections ideal for curved bridges and segmental bridge construction;
- a large span-to-depth ratio;
- structural stability and good aesthetic appearance due to monolithic construction; and
- a hollow inside portion of the concrete, which provides a space for utilities such as gas lines, water pipes, telephone ducts, storm drains, and sewers.

However, a lack of adequate transverse force results in differential movement between the adjacent box beams, which can lead to the formation of longitudinal cracks in the deck slabs as shown in **Fig. 3**. Seepage of water and deicing salts through these cracks can result in corrosion of the steel reinforcement.

To eliminate the corrosion problems associated with conventional steel reinforcement and thereby considerably reduce the maintenance costs of structures, fibrous composite materials are a viable alternative. Some of the notable characteristics of composite materials—such as corrosion and weathering resistance, high strength- and stiffness-to-weight ratios, light weight, magnetic insensitivity, and ease of handling—have caused the emergence of FRPs as a high-potential future construction material in the highway bridge construction industry.[4]

Literature review

Some of the available literature related to flexural response and ductility of prestressed FRP concrete bridges is reviewed in this section.

Based on an experimental study consisting of scale models of beams prestressed with different types of carbon fibers, Fam et al.[5] concluded that beams prestressed with either

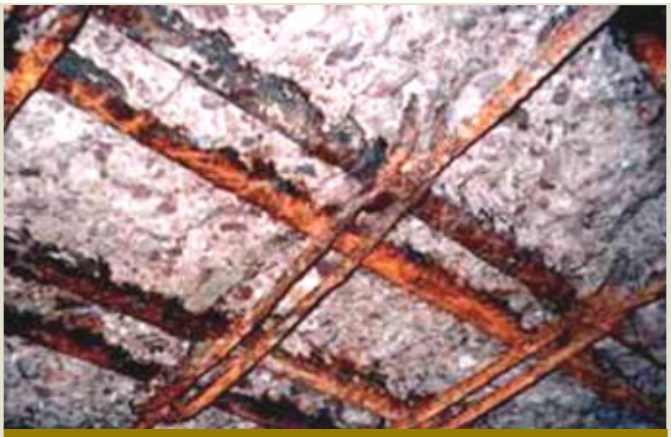

Figure 1. Shown is an example of steel-reinforcement corrosion.

Figure 2. This steel-reinforcement corrosion resulted after its concrete cover experienced spalling.

steel strands or carbon FRP (CFRP) tendons exhibited similar stiffness until the yielding of steel. Kakizawa et al.[6] observed that in the case of beams with CFRP that was partially prestressed, most of the flexural cracks were concentrated at midspan, whereas fewer cracks were observed in the case of fully prestressed and ordinary reinforced beams. Naaman et al.[7] evaluated T-beams partially prestressed with CFCC strands and reported that the nonprestressed reinforcement imparted residual strength and ductility to the structure. Theriault and Benmokrane[8] investigated the dependency of the reinforcement ratio ρ and compressive strength of concrete f_c' on the flexural behavior of CFRP bars. They found that crack width and crack length decreased with an increase in reinforcement ratio ρ, whereas the stiffness of the beam was directly proportional to the reinforcement ratio.

Based on a study on the flexural characteristics of concrete beams prestressed with bonded and unbonded CFRP tendons, Kato and Hayashida[9] concluded that the failure of bonded CFRP prestressed concrete beams was brittle, whereas the beams prestressed with unbonded CFRP

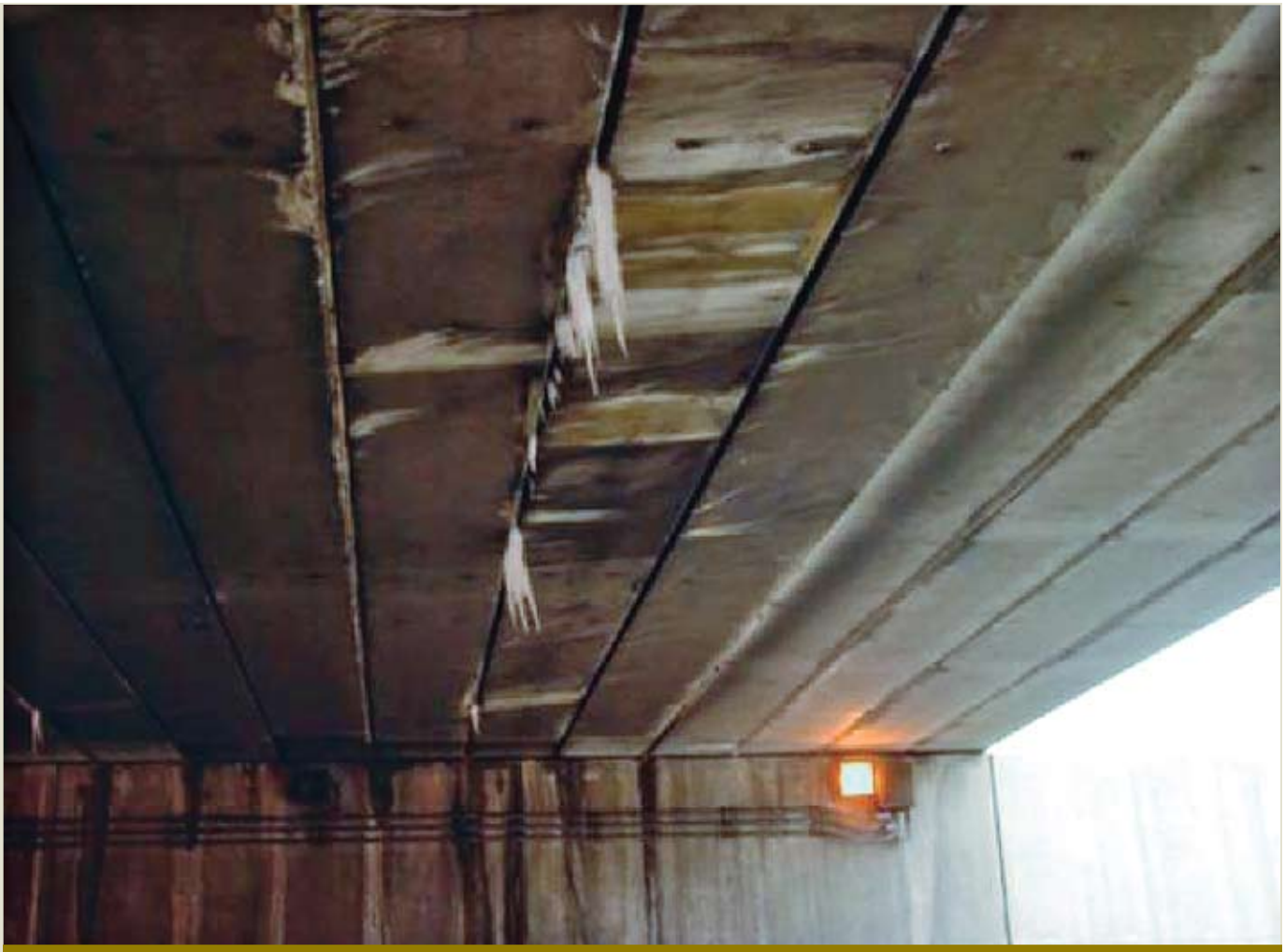

Figure 3. Water that has formed icicles can easily infiltrate longitudinal cracks that develop between adjacent box beams.

tendons had roughly the same degree of ductility as did the beams reinforced with steel strands. They also determined that the prestress level was the only factor in determining the cracking load other than concrete compressive strength.

Maissen and De Semet[10] evaluated the comparative response of concrete beams prestressed with bonded and unbonded CFRP tendons and beams prestressed with bonded steel strands. They concluded that the beams prestressed with bonded and unbonded CFRP tendons demonstrated a higher flexural load-carrying capacity than the beams prestressed with bonded steel strands demonstrated.

Grace and Sayed[11] studied the flexural behavior of double-tee-beam bridges prestressed internal (bonded) and external (unbonded) post-tensioning CFCC strands with and without repeated load effects. They concluded that repeated load had no significant effect on the external post-tensioning CFCC strands. Recently, Ng[12] experimentally and theoretically examined the tendon stress and flexural strength of externally prestressed beams and concluded that the span of the beam had no significant effect on the stress increase in external tendons. This result contradicts the concluding remarks of Naaman and Alkhairi.[13]

According to an investigation conducted on the structural ductility of concrete beams prestressed with aramid FRP (AFRP), CFRP, and steel strands, Naaman and Jeong[14] concluded that the beams prestressed with FRP tendons experienced lower ductility than the beams prestressed with steel strands. Moreover, they proposed a new approach to calculate the ductility that is applicable to both steel and FRP reinforced/prestressed structures.

Grace et al.[15,16] proposed a new construction approach for multispan, prestressed, CFRP concrete bridges. It was demonstrated that external post-tensioning using continuous draped tendons, continuous CFRP reinforced deck slab, and transverse post-tensioning enhanced the ductility of the bridge model. Taniguchi et al.[17] examined the flexural response of concrete beams prestressed with CFRP and AFRP tendons and concluded that the use of CFRP as transverse reinforcement increased the ductility of the beams.

Iwamoto et al.[18] suggested that the flexural behavior and ultimate strength of prestressed FRP concrete could be estimated by a conventional prestressed concrete analysis. To account for the effect of multiple layers of bonded prestressing and unbonded post-tensioning reinforcement,

Grace and Singh[19] conducted a parametric study using a nonlinear computer program based on the strain-controlled approach. These researchers concluded that the ultimate flexural strength and failure modes of double-tee beams prestressed with multilayered pretensioning and external post-tensioning CFRP tendons depend on the level of initial pretensioning and post-tensioning forces.

The objective of this paper's investigation is to construct, instrument, and test three precast, prestressed concrete box-beam bridge models reinforced with bonded pretensioning and unbonded post-tensioning CFCC strands. **Figure 4** illustrates the details of these models. The parameter considered in this investigation was the effect of unbonded, longitudinal post-tensioning on the flexural behavior of the bridge models. The investigation also addresses transfer lengths of CFCC strands, load-deflection and load-strain responses of the bridge models, and the ultimate load-carrying capacities, ductility, and failure modes of the three models.

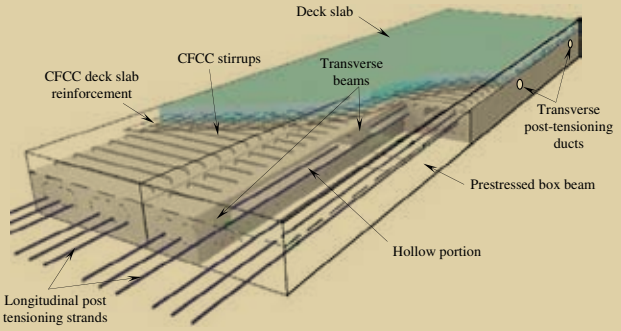

Figure 4. This typical box-beam bridge model is reinforced and prestressed with CFCC. Note: CFCC = carbon-fiber-composite cable.

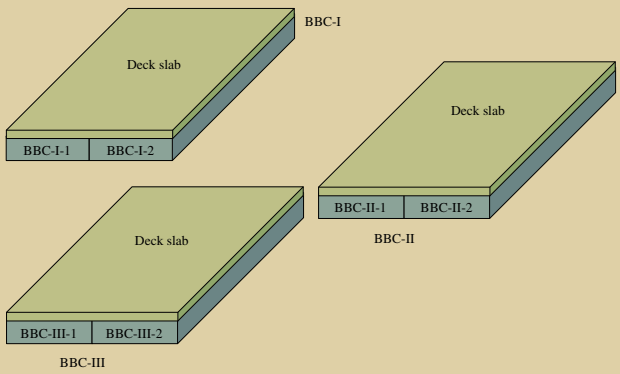

Figure 5. Shown are the designations for the adjacent box beams that comprise specimens BBC-I, BBC-II, and BBC-III.

Construction details

Construction of the box beams

Three box-beam bridge models, each consisting of a pair of precast, prestressed concrete box beams, were constructed. **Figure 5** shows the three bridge models, designated as BBC-I, BBC-II, and BBC-III, which differ in the arrangement and forces in the unbonded, longitudinal post-tensioning strands. The box beams used in the construction of the bridge models were 20 ft (6.1 m) long, 38 in. (970 mm) wide, and 9 in. (230 mm) deep.

The cross section, longitudinal section, and dimensions were the same for the three models. BBC-I was constructed with unbonded longitudinal strands, whereas BBC-II did not contain unbonded, longitudinal post-tensioning strands. BBC-III contained unbonded longitudinal strands with zero post-tensioning force, and their prestressing heads were anchored at both ends of the bridge model. **Figures 6** and **7** show the cross-sectional details of bridge models before casting a 3-in.-thick (75 mm) concrete deck slab.

Each box beam incorporated two hollow, rectangular voids in the longitudinal direction. Each void was 12 in. (300 mm) wide and 4 in. (100 mm) deep in cross section. In addition, each box beam was constructed with four rectan-

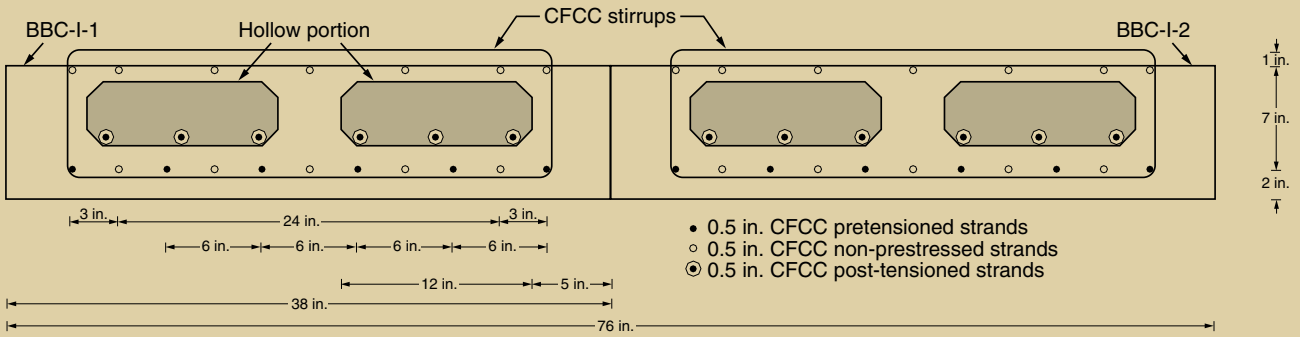

Figure 6. This drawing shows the cross-section details of adjacent box beams for BBC-I and BBC-III without the deck slab. Note: CFCC = carbon-fiber-composite cable. 1 in. = 25.4 mm.

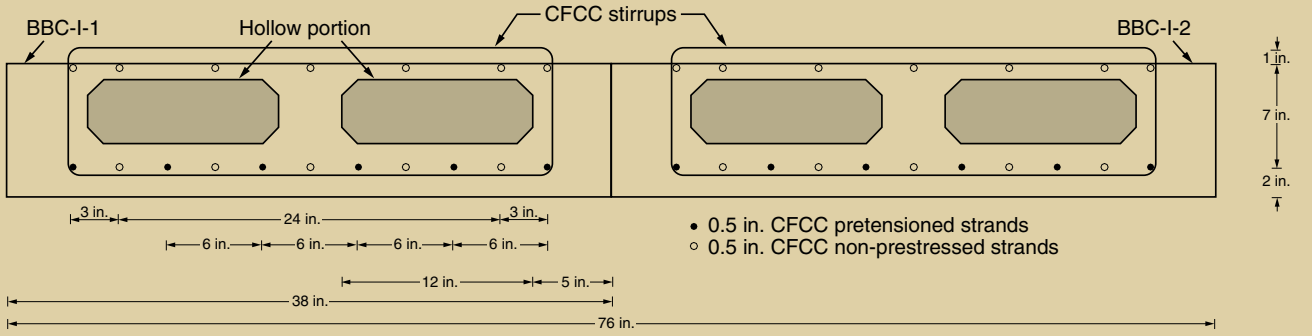

Figure 7. This drawing shows the cross-section details of adjacent box beams for BBC-II without the deck slab.
Note: CFCC = carbon-fiber-composite cable. 1 in. = 25.4 mm.

gular transverse diaphragms, one at each end of the beam and two at intermediate sections symmetrically located at one-third distance along the span of the beams. Unbonded, transverse post-tensioning of each bridge model was performed at these transverse diaphragm locations.

The construction of each box beam included the preparation of CFCC reinforcement cages, as shown in **Fig. 8**. Each reinforcement cage consisted of seven pretensioned bottom strands, four nonprestressed bottom strands, and seven nonprestressed top strands. The nonprestressed top strands were provided to prevent cracking due to shrinkage stresses and handling operations.

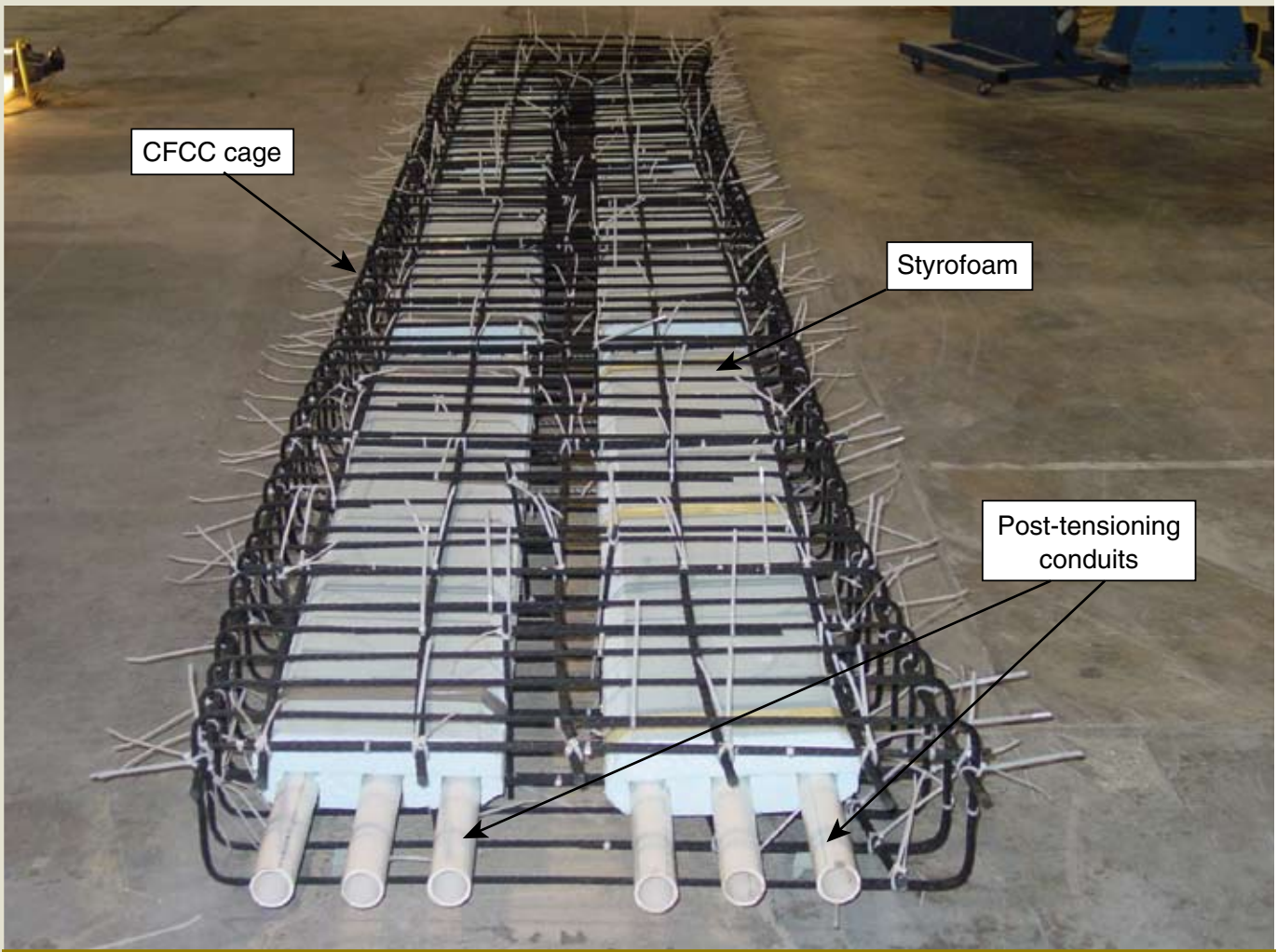

Figure 8. This CFCC cage with styrofoam provided the reinforcement and shape for BBC-I. Note: CFCC = carbon-fiber-composite cable.

Table 1. Properties of CFCC 7-wire strands and stirrups used in the bridge

Material characteristics	Type of strand		
	Stirrups	Strands	Deck slab reinforcement
Standard diameter *d*, in.	0.3	0.49	0.3
Measured diameter, in.	0.33	0.50	0.33
Effective cross-sectional area, in.^{2}	0.047	0.12	0.047
Pitch, in.	3.3	6.1	3.4
Linear density, lb/ft	0.0437	0.102	0.0437
Guaranteed breaking load, kip	12.8	31.9	12.8
Standard guaranteed strength, ksi	272.0	271.0	272.0
Maximum value of measured breaking load, kip	16.0	42.2	16.0
Minimum value of measured breaking load, kip	14.6	40.7	15.1
Number of test specimens	5.0	8.0	5.0
Average measured breaking load, kip	15.1	41.1	15.5
Measured tensile strength, ksi	322.0	350.0	329.0
Measured elastic modulus, ksi	20,450.0	20,595.0	20,305.0
Maximum elongation, %	1.6	1.7	1.6

Note: CFCC = carbon-fiber-composite cable. 1 in. = 25.4 mm; 1 kip = 4.448 kN; 1 ksi = 6.985 MPa; 1 lb/ft = 1488 g/m.

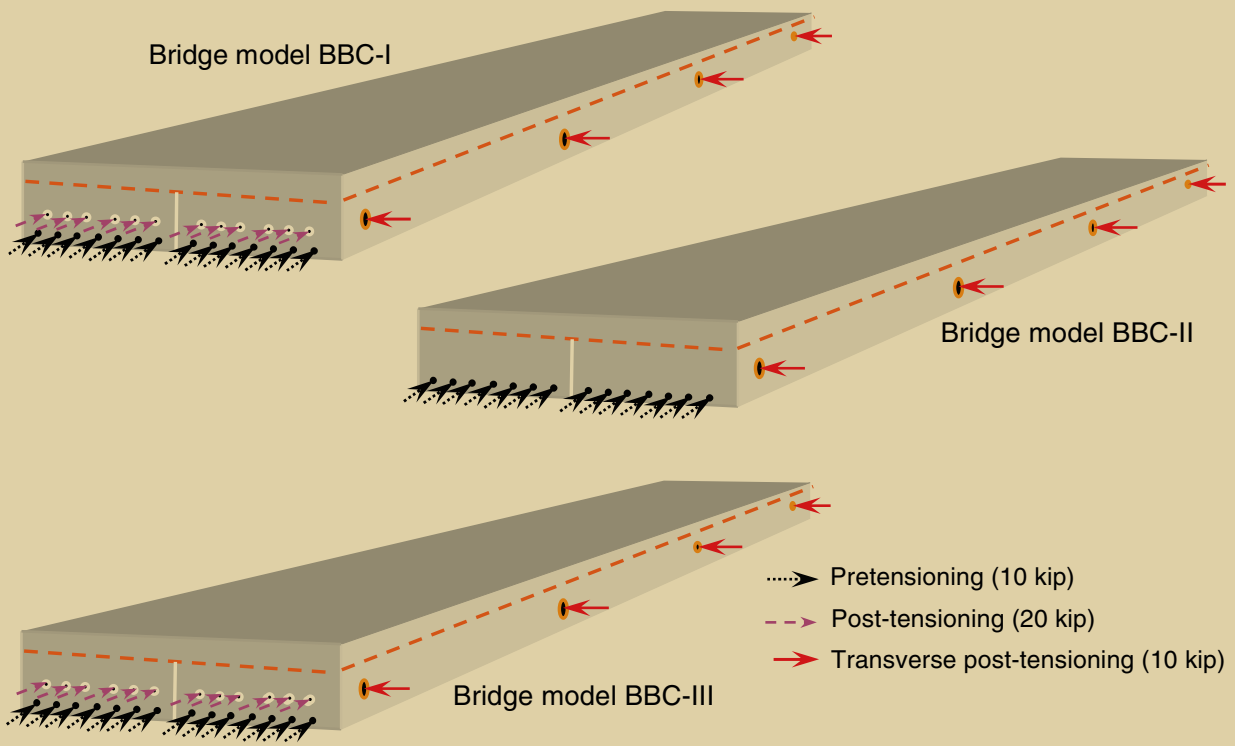

Figure 9. This schematic representation shows the location and amount of prestressing forces used for longitudinal and transverse post-tensioning. Note: 1 kip = 4.448 kN.

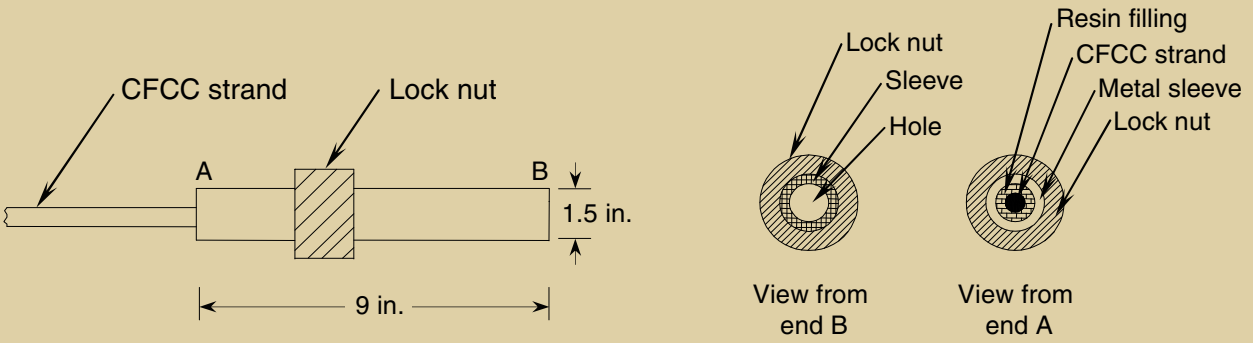

Figure 10. Shown are the anchorage details of CFCC strands used in the construction of the bridge models. Note: CFCC = carbon-fiber-composite cable. 1 in. = 25.4 mm.

CFCC shear stirrups were provided at a spacing of 4 in. (100 mm) to avoid premature shear failure. **Table 1** shows the material properties of the CFCC strands and stirrups. Commercially available ties held the reinforcing cage together. Six and four polyvinyl chloride (PVC) conduits were provided in the longitudinal and transverse directions, respectively, for passing the unbonded post-tensioning strands. **Figure 9** shows the prestressing forces and their locations.

The reinforcement cages were placed inside wooden formwork. Strain gauges were installed on the pretensioning strands before placing concrete in the formwork. To provide the required concrete cover of 2 in. (50 mm) at the bottom of each beam, 4 in. (100 mm) circular plastic supports were added to the formwork.

Figures 10 and **11** show the prestressing system, which consisted of a long-stroke, center-hole jack, a hydraulic pump with pressure gauge, a prestressing chair, a threaded steel tensioning rod, and a coupler. In BBC-I, each pretensioned CFCC strand was stressed to an average force of 9.95 kip (44.3 kN), thus constituting 69.7 kip (310 kN) of total pretensioning force for each box beam. The jacking force was monitored with the hydraulic pump's pressure

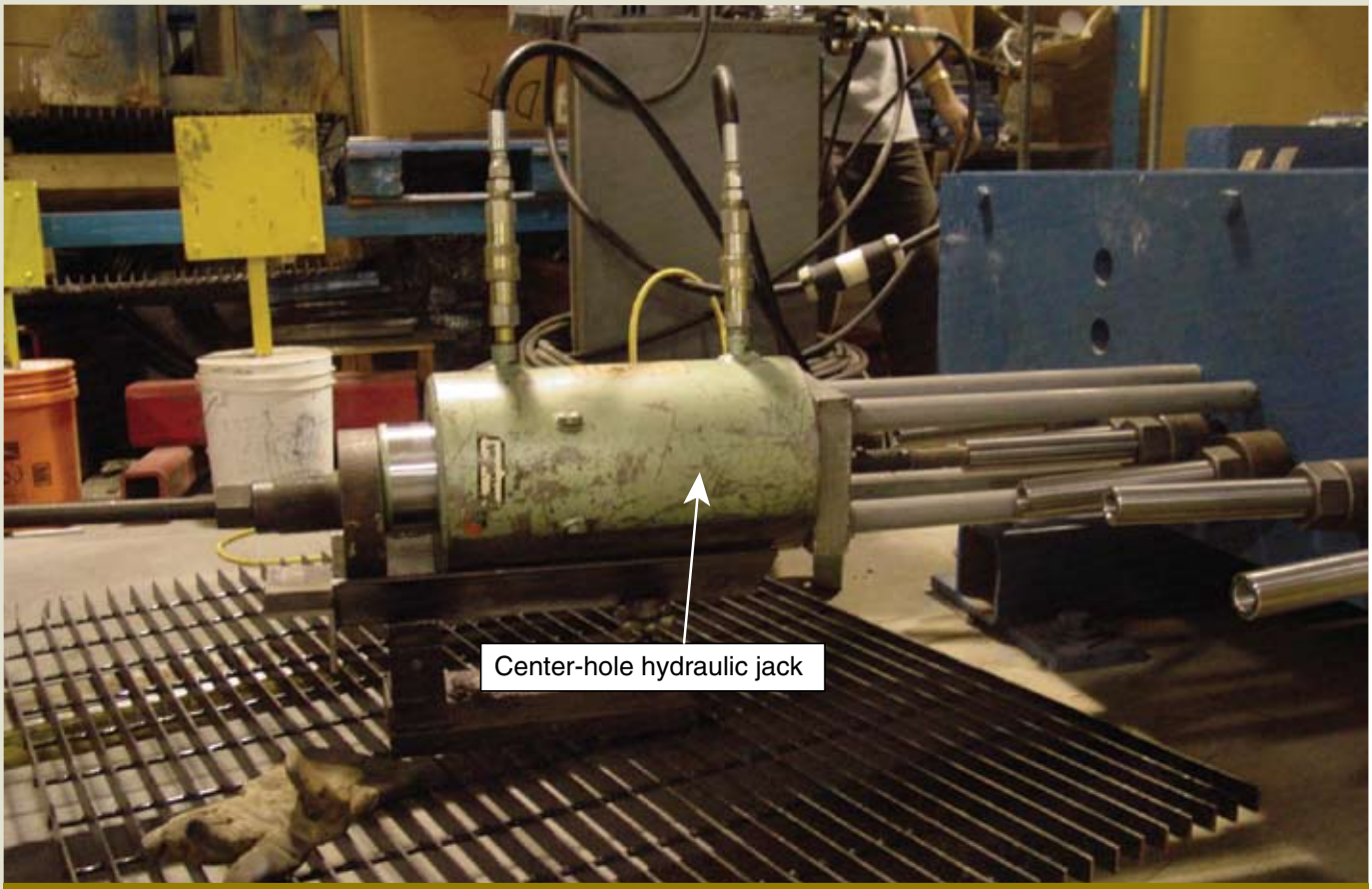

Figure 11. The carbon-fiber-composite cable strands were pretensioned using a center-hole hydraulic jack.

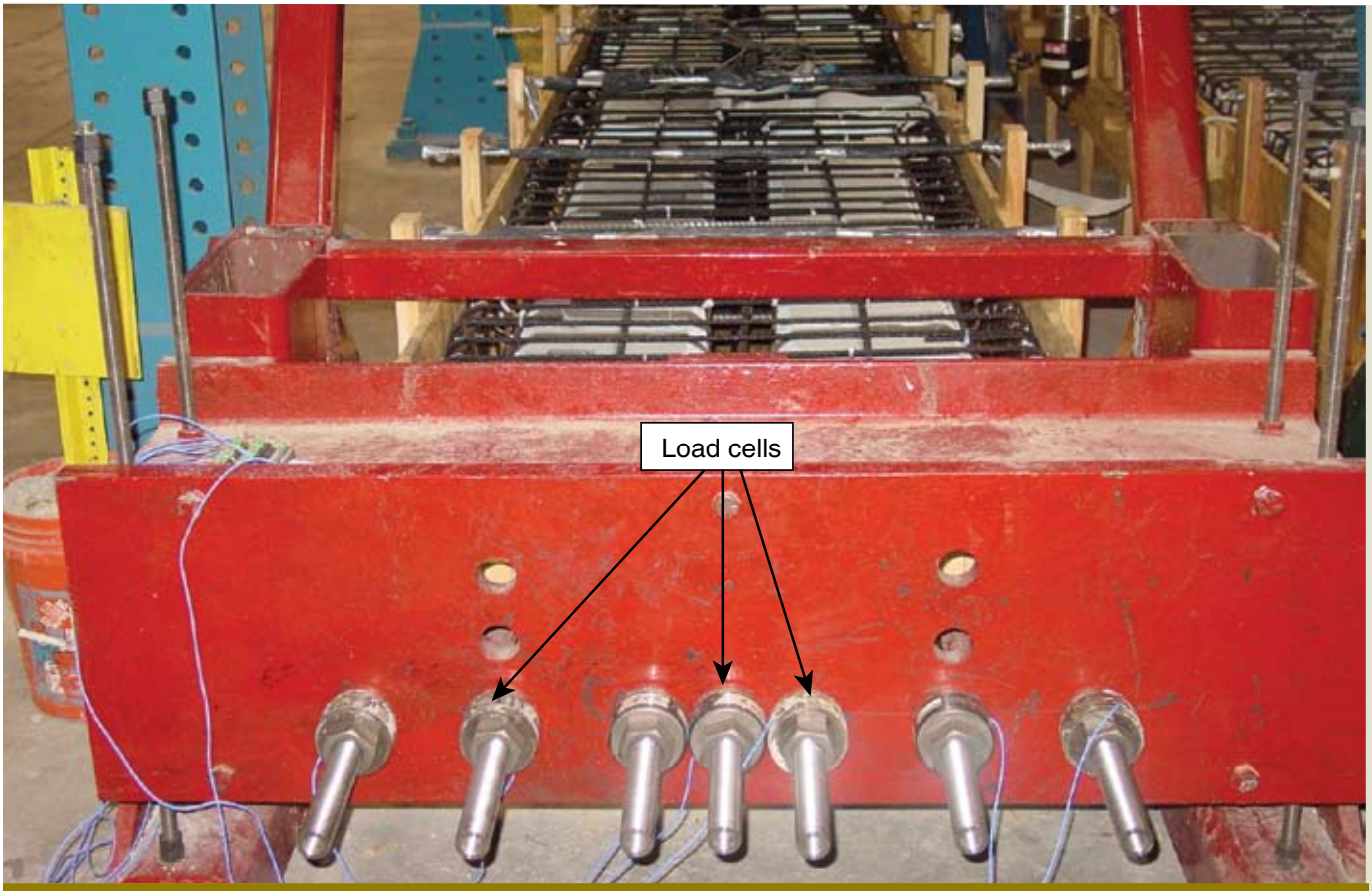

Figure 12. The load cells were placed at bulkhead dead ends of the prestressing strands, which aided the hydraulic pump pressure gauge in monitoring the jacking force applied to the box beams.

gauge and the load cells placed at the dead end of the prestressing strands (**Fig. 12**).

After the CFCC strands were prestressed, concrete was placed inside the formwork. The stirrups protruded beyond the top flange of the box beams to provide shear connection with the deck slab. The box beams were wet cured with water-soaked burlap for seven days. When the concrete attained the desired compressive strength, the strands were cut to transfer the pretensioning forces to the concrete from both ends of the box beams simultaneously.

The 28-day concrete compressive strengths of the precast concrete beams for BBC-I, BBC-II, and BBC-III were 8.3 ksi (57 MPa), 8.1 ksi (56 MPa), and 7.9 ksi (55 MPa), respectively.

Construction of bridge models

Individual precast, prestressed concrete box beams were moved to the testing area underneath the loading frame and were placed adjacent to each other with simple supports at their ends. **Figure 13** shows the gap between the two adjacent box beams in each bridge model being filled with structural concrete. After the filler concrete was cured, an initial transverse post-tensioning force was applied in each of the four transverse post-tensioning strands passing through the corresponding transverse diaphragms of the box beams (**Fig. 14**). The transverse post-tensioning was necessary to maintain the structural integrity of the two adjacent box beams and to prevent any differential movement during longitudinal post-tensioning, casting of the deck slab, and application of external loads.

Figure 13. A graduate student fills the gap between adjacent box beams of a bridge model with concrete.

Figure 14. A bridge model receives an initial transverse post-tensioning force, which was necessary to maintain the structural integrity of the two adjacent box beams and to prevent any differential movement during longitudinal post-tensioning, casting of the deck slab, and application of external loads.

Initial transverse post-tensioning consisted of 50% (10 kip [45 kN]) of the design transverse post-tensioning force per strand. After initial transverse post-tensioning, an initial longitudinal post-tensioning force was applied in the unbonded longitudinal strands of BBC-I (**Fig. 15**). About 10% of the design post-tensioning force was used for each strand—20 kip (89 kN). The final transverse and longitudinal post-tensioning forces were applied after construction of the CFCC-reinforced deck slab was completed.

Construction of deck slab

For deck-slab reinforcement, square grids of 0.3-in.-diameter (8 mm) strands were fabricated at a constant spacing of 8 in. (200 mm). **Figure 16** shows the reinforcement grid placed over the box beams and tied to the protruding stirrups. **Figure 17** shows the placement of the 3-in.-thick (75 mm) deck slab.

The 28-day compressive strengths of deck-slab concrete for BBC-I, BBC-II, and BBC-III were 6.2 ksi, 7.9 ksi, and 6.2 ksi (43 MPa, 55 MPa, and 43 MPa), respectively. The final transverse and longitudinal post-tensioning forces, which constitute about 50% and 90% of the design post-tensioning forces, respectively, were applied after the deck-slab concrete attained the desired compressive strength.

Instrumentation and test setup

Demountable mechanical (DEMEC) strain gauges measured concrete strain at the two ends of the box beams to determine the transfer lengths at the time of prestress transfer to the concrete. Measurements were taken before and after the release of pretensioning forces using a DEMEC strain gauge with a precision of 5×10^{-5} in. (130×10^{-5} mm).

Strain gauges installed on the top surface of the deck slab at midspan measured the strain of concrete during external loading. Strain gauges at the top surface were symmetrically placed about the longitudinal mid-axis of the bridge models. The nonprestressed strands located at the tops and bottoms of the box beams were instrumented with strain gauges to determine their behavior during loading of the

Figure 15. Shown are the adjacent box beams for BBC-I prior to constructing its deck slab after initial post-tensioning of longitudinal and transverse unbonded strands.

Figure 16. This carbon-fiber-composite cable reinforcement cage made from square grids of 0.3-in.-diameter (7.5 mm) strands at a constant spacing of 8 in. (200 mm) was the deck-slab reinforcement.

Figure 17. The concrete deck slab was placed over two adjacent box beams for one of the bridge models.

bridge models. Linear motion transducers installed at mid-span monitored the bridge deflection. Load cells installed at the dead end of the longitudinal and transverse post-tensioning strands measured the post-tensioning forces in these strands. All of the measuring devices and sensors were interfaced with the data-acquisition system during the load tests of the bridge models.

Test setup

A four-point loading frame was used to test each bridge model in flexure. The frame was placed at the center of the bridge model with each of the two loading points placed at the centerline of each box beam. The four-point loading frame simulated a standard truck loading, and its dimensions ensured flexural failure of all bridge models under investigation. Prior to application of the ultimate load cycle, each bridge model was subjected to several static loading and unloading cycles at a uniform rate of about 6 kip/min (27 kN/min). The purpose of conducting these loading cycles was to separate the elastic and inelastic energies under the load-deflection curve so that the ductility could be evaluated based on energy concept.[20,21]

Results and discussion

Several characteristics of the bridge models were compared: transfer length; load-deflection response; load-strain response in the strands; forces in longitudinal and transverse unbonded, post-tensioned strands; energy ratios as a measure of bridge ductility; and modes of failure.

Transfer length

Experimentally obtained transfer lengths were compared with three existing transfer-length equations. DEMEC strain gauges placed at the level of the pretensioned strands at both ends of each beam measured the transfer lengths L_t of the 0.49-in.-diameter (13 mm) CFCC strands used for pretensioning the box beams.

After the concrete had cured for seven days, the prestressing forces were released. At the time of release, the compressive strengths of concrete for BBC-I, BBC-II, and BBC-III were 5.1 ksi (35 MPa), 6.2 ksi (43 MPa), and 6.3 ksi (43 MPa), respectively. DEMEC strain-gauge readings were taken before and after the release of prestressing forces. The linear strain profile at both ends

along the span was plotted, and the 95% of average maximum strain method[22] was applied to obtain the transfer length from the plotted strain profile. In this method, a line both parallel to the beam span and passing through 95% of average maximum strain is drawn. Distance from the point of intersection of this horizontal line with the straight-line profile of strains at both live and dead ends to the corresponding end faces gives transfer lengths at the corresponding ends.

Figure 18 shows the typical transfer length of the box beams at transfer of prestress. Table 2 compares the experimental values of transfer length with the theoretical values obtained from the three existing equations,[22–24] which are expressed as Eq. (1), (2), and (3), respectively.

$$L_t = \frac{f_{pi} d_b}{\alpha_t f_{ci}'^{0.67}} \text{ (mm)} \quad (1)$$

$$L_t = \frac{f_{pi} d_b}{20} \text{ (mm)} \quad (2)$$

$$L_t = \frac{480 d_b}{\sqrt{f_{ci}'}} \text{ (mm)} \quad (3)$$

where

f_{pi} = prestress at transfer, MPa

d_b = nominal diameter of the strand/tendon, mm

α_t = 2.12

= transfer length coefficient for CFCC strands

f_{ci}' = concrete compressive strength at prestress transfer, MPa

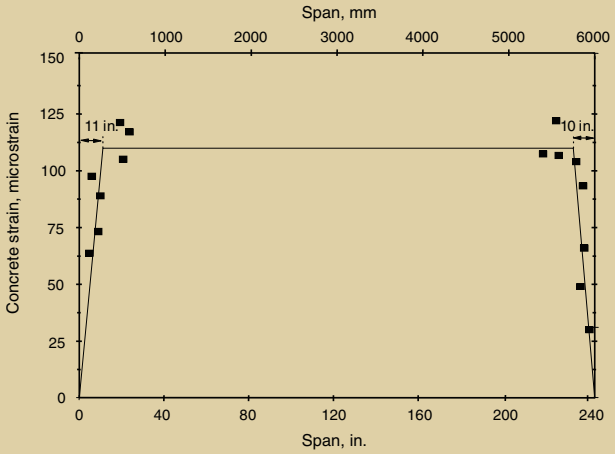

Figure 18. Shown are typical transfer lengths of box beams at the transfer of prestress. Note: 1 in. = 25.4 mm.

The measured transfer-length readings ranged from 10 in. to 15 in. (250 mm to 380 mm), with an average value of 12.5 in. (318 mm). In terms of nominal strand diameter d_b, the measured transfer length was in the range of $20d_b$ to $30d_b$ with an average value of $25d_b$.

The transfer lengths obtained from the Grace[22] and ACI 318[23] equations were close to the experimental values, whereas Zou's[24] equation overestimated the transfer lengths. The average transfer length obtained from the ACI 318 equation was 14.3 in. (360 mm), which was 14.4% greater than the experimental values. The average transfer length obtained from the Grace equation was 11.3 in. (290 mm), which was 9.6% less than the experimental values.

The Grace equation predicted more realistic values, which matched closely with the test results because it takes into account the average prestressing level in the strands f_{pi} as well as the concrete strength at prestress transfer f_{ci}'. Although the ACI 318 equation provided acceptable results,

Table 2. Measured and calculated transfer lengths of carbon-fiber-composite cable pretensionng strands for BBC-I, BBC-II, and BBC-III

Bridge model	Box beam	Average prestress in strand at transfer L_{pi}, ksi	Concrete strength at transfer f_{ci}', ksi	Measured transfer length L_t, in.			Calculated transfer length L_t, in.		
				Live end	Dead end	Average	Eq. (1)	Eq. (2)	Eq. (3)
BBC-I	BBC-I-1	82.0	6.1	11	10	10.5	10.7	13.9	36.4
	BBC-I-2	81.3		11	12	11.5	10.6	13.8	36.4
BBC-II	BBC-II-1	81.8	6.2	12	14	13.0	10.6	13.9	36.2
	BBC-II-2	85.2		13	11	12.0	11.0	14.5	36.2
BBC-III	BBC-III-1	86.5	6.3	13	12	12.5	11.1	14.7	35.9
	BBC-III-2	86.6		15	14	14.5	11.1	14.7	35.9

Note: 1 in. = 25.4 mm; 1 ksi = 6.985 MPa.

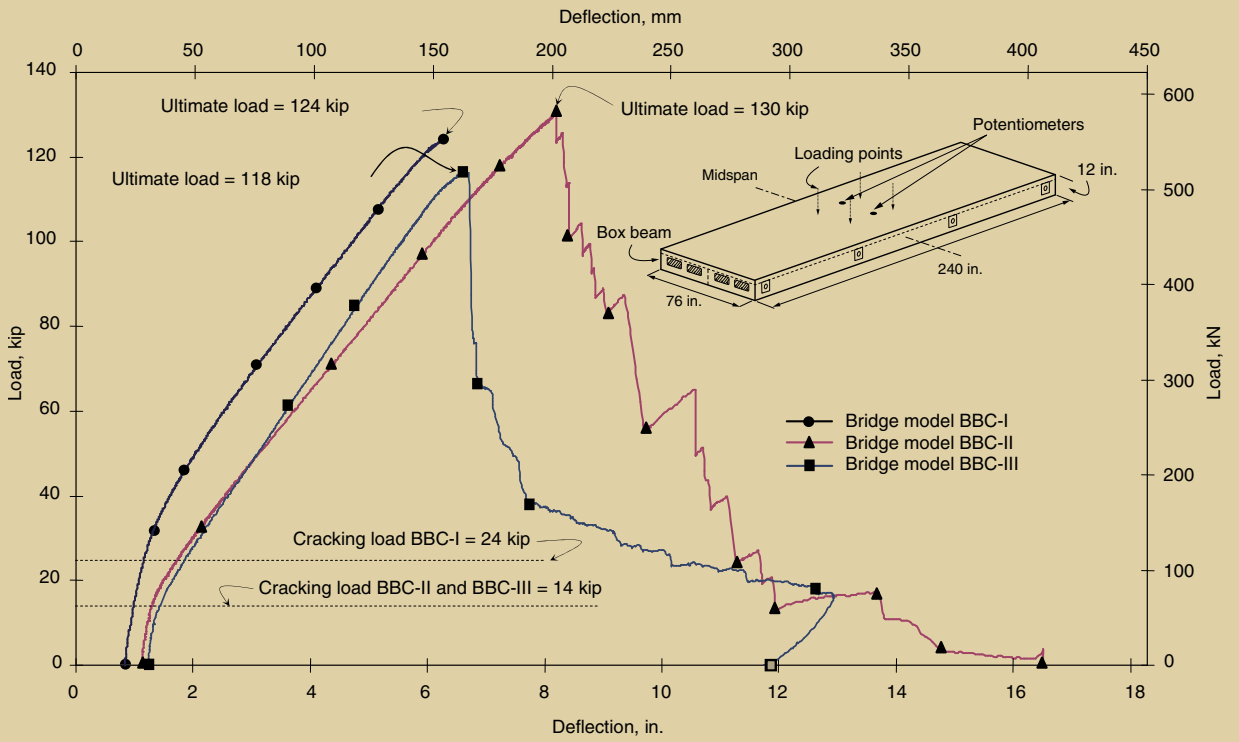

Figure 19. This graph depicts the ultimate load-deflection responses of BBC-I, BBC-II, and BBC-III. Note: 1 in. = 25.4 mm; 1 kip = 4.448 kN.

it disregards the effect of concrete strength and therefore does not match as closely with the test results as the Grace equation.

Load-deflection response

The midspan deflections of the simply supported bridge models were used to plot the load-deflection curves. The load was applied monotonically until cracking, and it was applied in a cyclic fashion after the cracking stage until ultimate strength was met. The cumulative residual deflections for all of the previous static loading cycles provided the initial deflection for the ultimate load-cycle test. The cumulative residual deflections for BBC-I, BBC-II, and BBC-III were 0.78 in. (20 mm), 1.1 in. (28 mm), and 1.2 in. (30 mm), respectively.

Figure 19 presents the load-deflection responses obtained from ultimate loading cycles for bridge models. The slope of the load-deflection curve changed after cracking of the bridge models. The ultimate deflections for BBC-I, BBC-II, and BBC-III were 6.15 in. (156 mm), 8.1 in. (205 mm), and 7.3 in. (184 mm), respectively. The lesser ultimate deflection of BBC-I compared with that of BBC-II and BBC-III was attributed to the additional post-tensioning forces applied to BBC-I. In general, the ultimate deflections of the three bridge models were inversely proportional to the total prestressing forces—including pretensioning and longitudinal post-tensioning—applied to the corresponding bridge model, which signified that the prestressing helped reduce deflection and thus enhanced the serviceability of the structure.

Load-strain response

The load-strain response of extreme compression fibers has a vital role in determining failure modes of members, especially in over-reinforced members. In under-reinforced concrete beams, the load-strain responses of bottom pretensioning strands indicate the initiation of failure.

Strain in extreme concrete fiber The strain gauges installed at the tops of the deck slabs at midspan monitored the compressive strain in the concrete. The compressive strain in the concrete in response to the applied load was similar for the three bridge models. BBC-I and BBC-III exhibited compression failure, and the ultimate compressive strain in the extreme concrete fibers corresponding to the failure of BBC-I and BBC-III was 0.00310 and 0.00322, respectively. Alternatively, BBC-II exhibited tension failure, and the concrete compressive strain corresponding to the maximum load was 0.00304. **Figure 20** shows the average concrete compressive strains at the tops of the deck slabs at midspan for BBC-I, BBC-II, and BBC-III.

Strain in pretensioned strands The average initial strain in the pretensioned strands due to the prestressing forces was about 0.0042. **Figure 21** presents the strain in

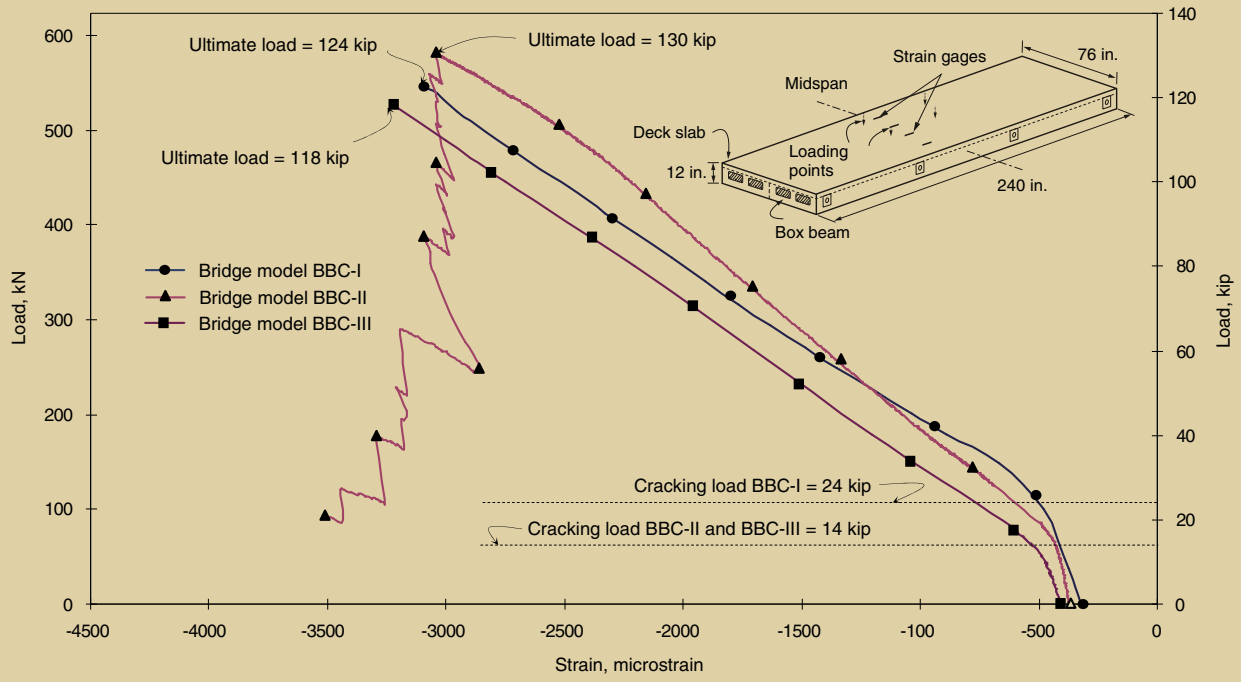

Figure 20. Shown are the average concrete compressive strains at midspan on the deck-slab tops of BBC-I, BBC-II, and BBC-III. Note: 1 in. = 25.4 mm; 1 kip = 4.448 kN.

the pretensioned strands of BBC-I, BBC-II, and BBC-III plotted against the load. As mentioned previously, the bridge models were considered cracked after the first loading cycle. However, after unloading, the entire cross section of the bridge model was subjected to compressive stresses induced by the prestressing forces, which kept the cracks closed.

Under the ultimate load test and prior to the cracking load, an insignificant increase in the strain of the pretensioned strands was observed. However, after the cracks were opened, the bridge model started to behave as a cracked section, and the strain in the pretensioned strands increased significantly until failure. This increase was linear until the point of failure of strands by rupture.

The strain at rupture of the pretensioned strands for BBC-I and BBC-III was about 0.0118 and 0.0158 for BBC-II. The rupture strain of strand is rated at 0.017 by the manufacturer. For BBC-II, the rupture strain of the pretensioned strands was almost 93% of the rupture strain provided by the manufacturer. However, for BBC-I and BBC-III, the rupture strain was only 70% of the ultimate strain. These lower values were because concrete crushing controlled the failure.

Forces in unbonded, longitudinal post-tensioned strands

The stress increase in unbonded strands cannot be determined through the strain compatibility because of the lack of bond between the strands and the surrounding concrete.[13] Unlike bonded strands, the increase in flexural stress of unbonded strands is independent of the cross section and depends mainly on the deformation of the whole member. The center-hole load cells placed at the dead end of each unbonded longitudinal strand monitored the variations in forces in the unbonded, longitudinal post-tensioned strands of BBC-I and BBC-III.

For BBC-I, the unbonded longitudinal strands were post-tensioned with an average force of 20 kip (90 kN) per strand. To prevent sagging of the unbonded longitudinal strands of BBC-III, the strands were post-tensioned with an average force of 1 kip (4.5 kN) per strand. Both bridge models BBC-I and BBC-III demonstrated behavior similar to that of the unbonded, longitudinal post-tensioned strands.

Figure 22 shows the average increase in the unbonded longitudinal strand forces, which were 4.7 kip (21 kN) and 4.9 kip (22 kN) for BBC-I and BBC-III, respectively. This indicated that the increase in the forces in unbonded longitudinal strands was independent of the initial post-tensioning force. It was also observed that the unbonded

longitudinal post-tensioned strands remained intact even after the complete collapse of both bridge models.

Ductility of bridge models

Ductility is of great importance for the safety of structures, especially for those subjected to seismic loading conditions. Due to the lack of plastic behavior of CFRP strands, the conventional definition of ductility cannot be used to evaluate the ductility of bridges reinforced with prestressed CFRP strands. Ductility of FRP prestressed concrete sections can be evaluated by the ratio between the elastic and inelastic energies consumed under the load-deflection curve of the bridge.[20,21]

Each bridge model was subjected to five static loading/unloading cycles prior to the ultimate load test. The load-deflection envelope of these cycles was used to calculate the released elastic energy, as well as the inelastic energy absorbed by each bridge model. Equation (4) is the energy ratio method[21] used to evaluate the ductility of each bridge model.

$$\text{Total energy ratio} = \frac{E_{inelastic} + E_{inelastic(additional)}}{E_{total}} \quad (4)$$

where

$E_{inelastic}$ = inelastic energy absorbed by each bridge model

$E_{inelastic(additional)}$ = additional inelastic energy absorbed by the bridge model after the ultimate load

E_{total} = total energy absorbed by each bridge model

Figures 23, **24,** and **25** present the elastic energies and inelastic energies for BBC-I, BBC-II, and BBC-III, respectively. For BBC-I, the elastic energy and inelastic energy absorbed by the bridge were 350 kip-in. (39.6 kN-m) and 156 kip-in. (17.6 kN-m), respectively. This bridge model failed in compression followed by immediate rupture of the pretensioned strands. Therefore, there was no additional inelastic energy absorbed by the bridge after the ultimate load, which accounted for the relatively low energy ratio of 31.0%.

BBC-II experienced a progressive failure due to the sequential rupture of the pretensioned strands. This resulted in additional inelastic energy absorbed by the bridge model after the ultimate load. The elastic energy, inelastic energy, and additional inelastic energy absorbed by the bridge model were 481 kip-in. (54.4 kN-m), 149 kip-in. (16.8 kN-m), and 271 kip-in. (30.6 kN-m), respectively. The corresponding energy ratio was 46.6%.

The failure of BBC-III was initiated by the crushing of concrete at the top of the deck slab, followed by the rupture of the pretensioned strands. With continued loading after the ultimate load was reached, the bridge model experienced a gradual crushing of concrete starting at part of the deck slab and propagating throughout the entire cross section. The elastic energy, inelastic energy, and additional inelastic energy absorbed by the bridge model were 353 kip-in. (39.9 kN-m), 156 kip-in. (17.6 kN-m), and

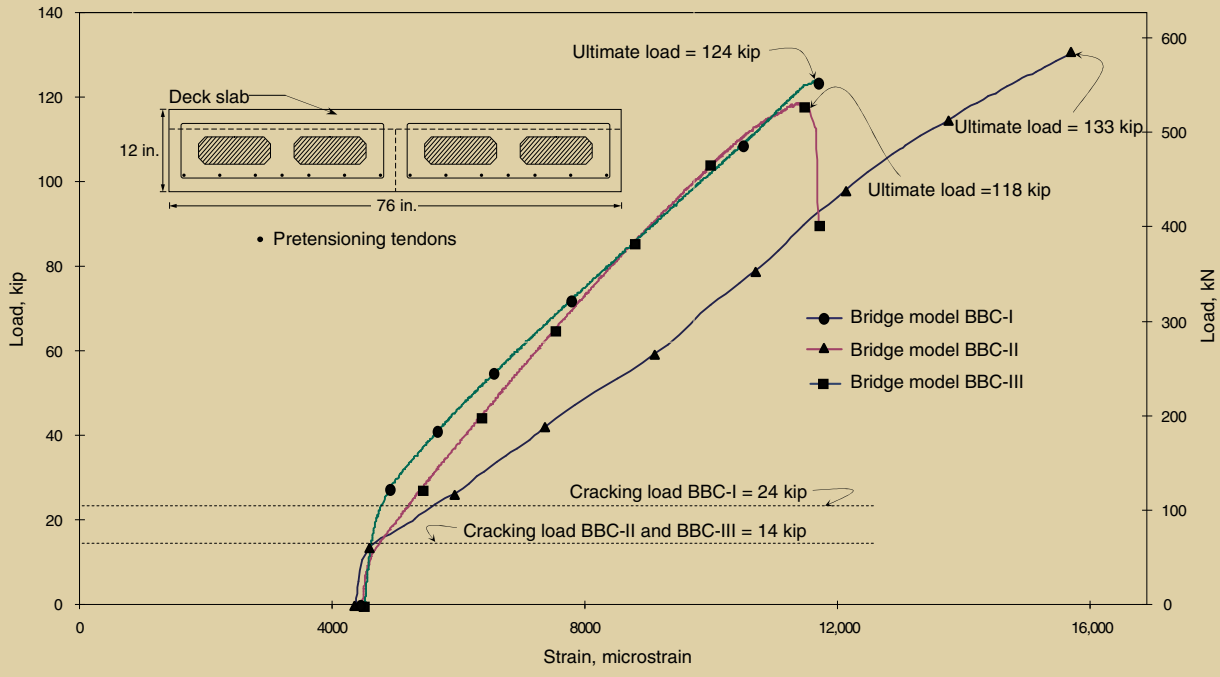

Figure 21. This graph shows strain response in the pretensioned strands of BBC-I, BBC-II, and BBC-III when subjected to the ultimate load test. Note: 1 in. = 25.4 mm.

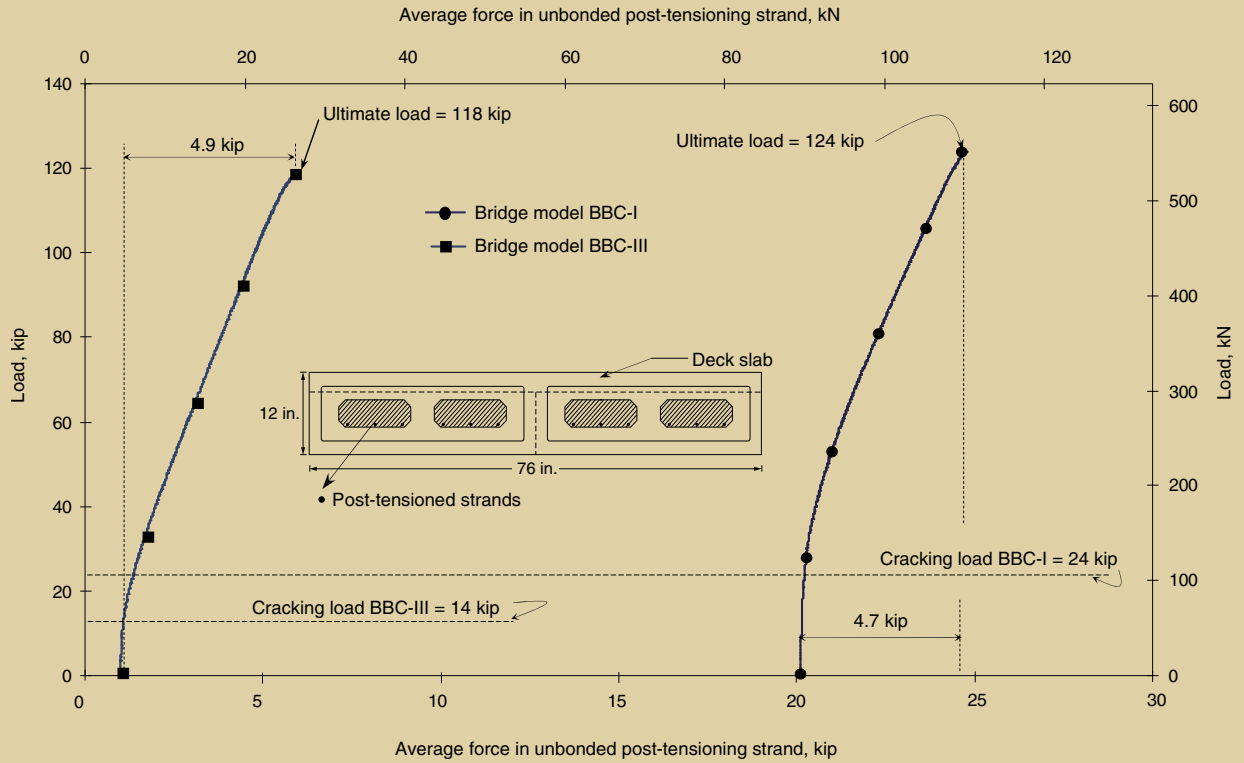

Figure 22. Shown is the average increase in forces due to loading for the unbonded longitudinal post-tensioned strands of BBC-I and BBC-III. Note: 1 in. = 25.4 mm; 1 kip = 4.448 kN.

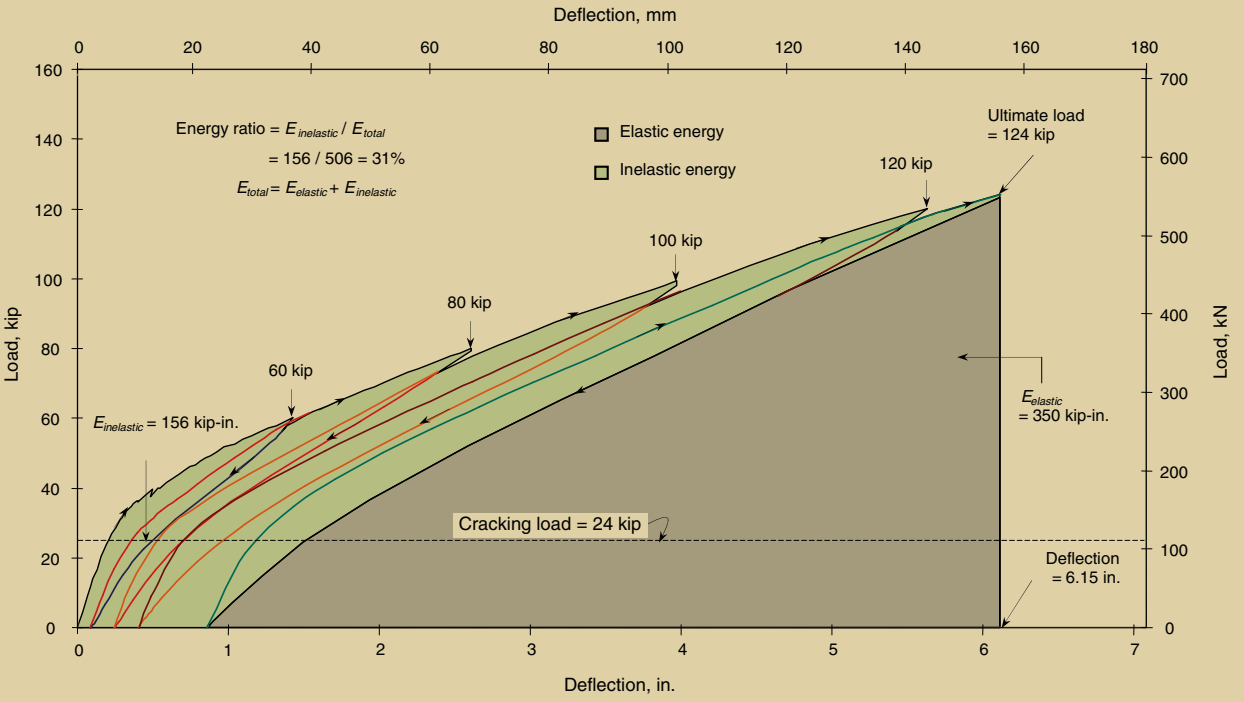

Figure 23. Shown are the elastic and inelastic energies for BBC-I. Note: 1 in. = 25.4 mm; 1 kip = 4.448 kN.

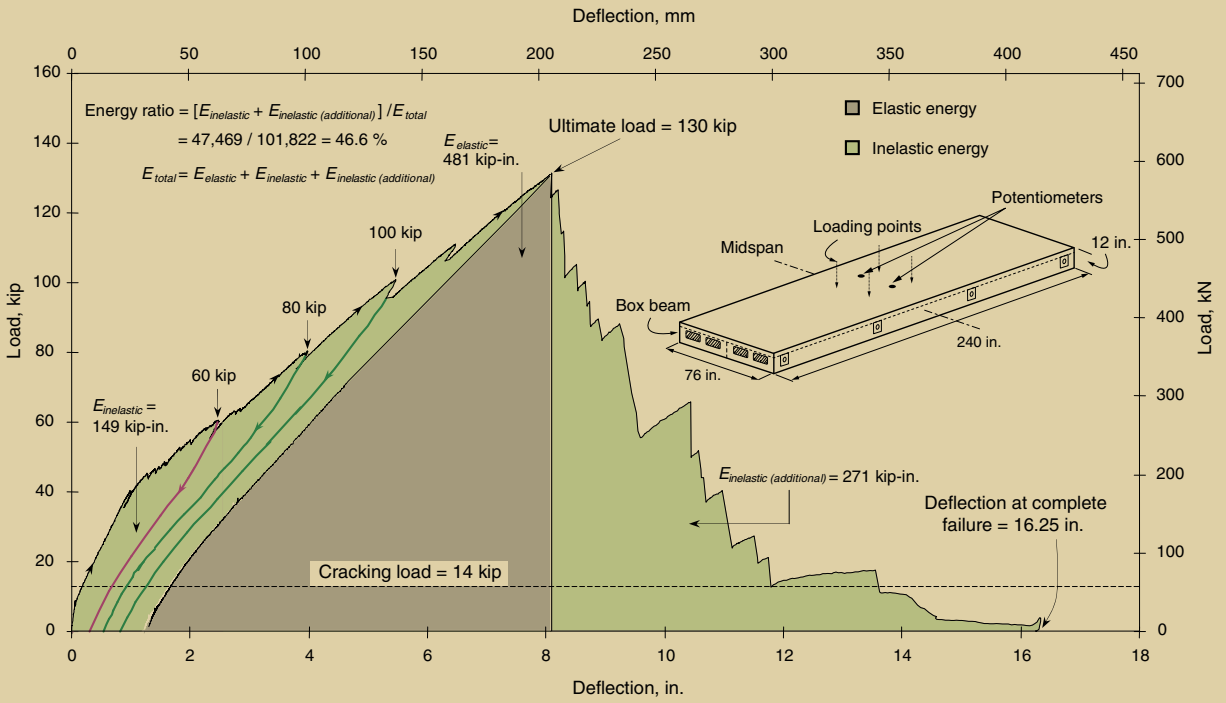

Figure 24. Shown are the elastic and inelastic energies for BBC-II. Note: 1 in. = 25.4 mm; 1 kip = 4.448 kN.

205 kip-in. (23.2 kN-m), respectively. The calculated energy ratio for BBC-III was 50.5%.

Failure of bridge models

As expected, the three bridge models experienced flexural failures. BBC-I was designed as an over-reinforced section. The failure of BBC-I started by the crushing of concrete at the extreme compression fiber at midspan, followed by the rupture of the pretensioned strands. A similar compression failure also occurred in BBC-III.

BBC-II was designed as an under-reinforced section. Hence, its failure began with the rupture of the pretensioned strands, which occurred progressively with a corresponding increase in the deflection of the bridge model. The cracks that developed in BBC-II and BBC-III were more intense than those developed in BBC-I. This was attributed to the greater level of prestressing provided for BBC-I due to the longitudinal post-tensioning forces. Although BBC-I had a greater level of total prestressing force than BBC-II had, the ultimate load-carrying capacity of BBC-I was 4.8% less. This was attributed to the lesser compressive strength of BBC-I's deck-slab concrete, which was about 22% less than that of BBC-II.

Conclusion

This research investigation primarily addressed the flexural performance of three concrete box-beam bridge models reinforced with prestressed CFCC, focusing on the effects of using unbonded longitudinal post-tensioning. Based on the results obtained from the investigation of BBC-I, BBC-II, and BBC-III, the following conclusions were drawn.

- When predicting the transfer length of pretensioning strands, the effect of prestress at transfer and the concrete strength should be considered. The average value of measured transfer lengths of 0.49-in.-diameter (12.5 mm) CFCC strands was $25d_b$, where d_b is the nominal diameter of strands. The average values of transfer lengths calculated by Grace,[22] ACI 318,[23] and Zou[24] are $23d_b$, $29d_b$, and $76d_b$, respectively. The experimental, Grace, and ACI 318 values were about 67% lower than those predicted by the Zou[24] equation, which did not take into account the effect of prestress at transfer.

- A greater level of total prestressing force prolongs the development of cracking and reduces the number and size of cracks that develop under loading. The cracking load for BBC-I was 24 kip (110 kN), while BBC-II and BBC-III both cracked at 14 kip (62 kN). The cracks that developed in BBC-I were fewer and less intense than those experienced by BBC-II and BBC-III.

- A greater level of total prestressing force reduces the amount of residual deflection. The cumulative midspan residual deflections due to the loading/unloading cycles for BBC-I, BBC-II, and BBC-III were 0.78 in. (20 mm), 1.10 in. (28 mm), and 1.2 in. (30 mm), respectively. BBC-I's lower deflection was

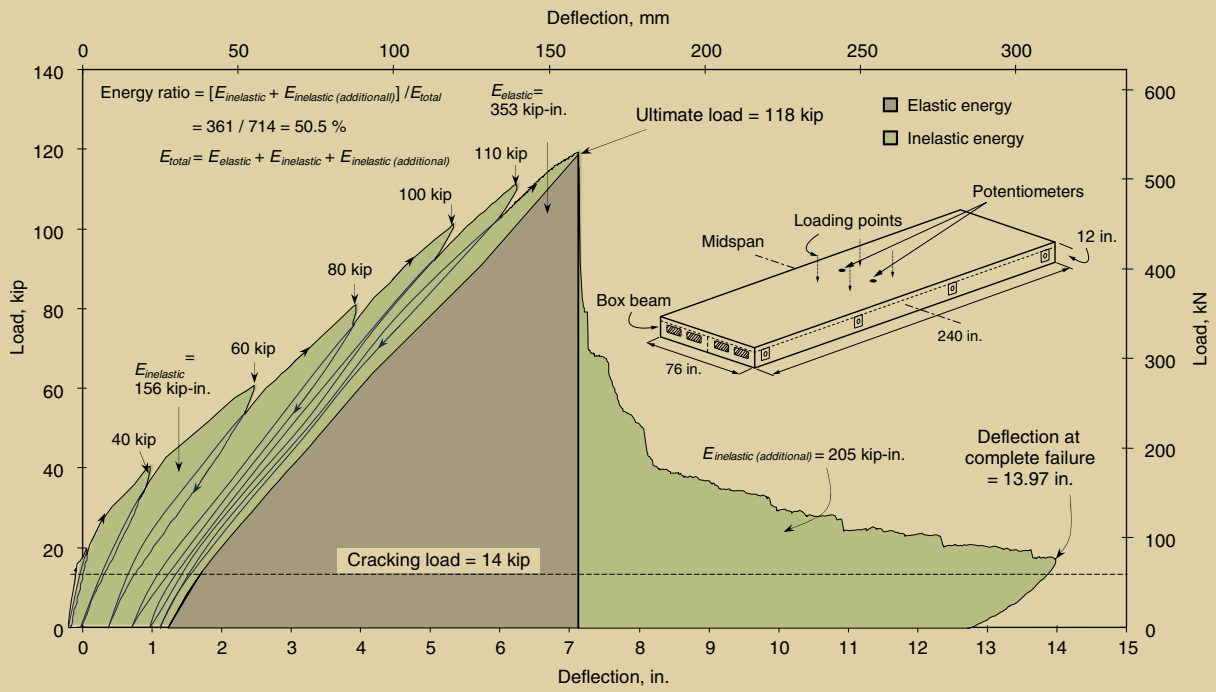

Figure 25. Shown are the elastic and inelastic energies for BBC-III. Note: 1 in. = 25.4 mm; 1 kip = 4.448 kN.

attributed to the higher prestressing forces from both the bonded pretensioned strands and unbonded post-tensioned strands.

- Designed as over-reinforced sections, BBC-I had a failure that was sudden, without significant warning prior to its failure, while failure of BBC-III was gradual. Thus, members with greater total prestressing force could fail suddenly.

- Prestressing strand is not used to its full potential when concrete structures fail in compression. The strain in pretensioned strands was bilinear until the point of failure by rupture. The measured failure strain of the pretensioned strands for BBC-II was about 0.0158, which was 93% of the rupture strain provided by the manufacturer. For BBC-I and BBC-III, the measured failure strains were both 0.0118, and both of these structures failed in compression.

- Greater amounts of inelastic energy are dissipated during progressive failures compared with failures that occur suddenly. Progressive failures accompany structures with lesser levels of total prestressing. The computed energy ratios (ductility indices) of BBC-I, BBC-II, and BBC-III were 31%, 46.6%, and 50.5%, respectively. BBC-I had a greater level of total prestress and failed suddenly, whereas BBC-II and BBC-III had lesser levels of prestress and failed progressively.

Acknowledgments

This investigation was supported by a consortium of the National Science Foundation (grant nos. CMS-0533260 and CMS-0408593), Tokyo Rope Manufacturing Co. Ltd. of Japan, the ACI Concrete Research Council, and Mitsui Co. of Japan. This study was possible due to the efforts of several research associates and graduate and undergraduate students.

References

1. El-Remaily, A., M. K. Tadros, T. Yamane, and G. Krause. 1996. Transverse Design of Adjacent Precast Prestressed Concrete Box Girder Bridges. *PCI Journal*, V. 41, No. 4 (July–August): pp. 96–107.

2. The National Bridge Inventory Study Foundation. 2004. *National Bridge Inventory (NBI) Report*. Washington, DC: Federal Highway Administration.

3. Taly, N. 1998. *Design of Modern Highway Bridges*. New York, NY: McGraw Hill Companies Inc.

4. American Concrete Institute (ACI) Committee 440. 2004. *Prestressing Concrete Structures with FRP Tendons (ACI 440.4R-04)*. Farmington Hills, MI: ACI.

5. Fam, A. Z., S. H. Rizkalla, and G. Tadros. 1997. Behavior of CFRP for Prestressing and Shear Reinforce-

ment of Concrete Highway Bridges. *ACI Structural Journal*, V. 94, No. 1 (January–February): pp. 77–86.

6. Kakizawa, T., S. Ohno, and T. Yonezawa. 1993. Flexural Behavior and Energy Absorption of Carbon FRP Reinforced Concrete Beams. In *SP-138: Fiber-Reinforced-Plastic Reinforcement for Concrete Structures—International Symposium*. Farmington Hills, MI: ACI.

7. Naaman, A. E., K. H. Tan, S. M. Jeong, and F. M. Alkahiri. 1993. Partially Prestressed Beams with Carbon Fiber Composite Cable Strands: Preliminary Tests on Strands. In *SP-138: Fiber-Reinforced-Plastic Reinforcement for Concrete Structures—International Symposium*. Farmington Hills, MI: ACI.

8. Theriault, M., and B. Benmokrane. 1998. Effects of FRP Reinforcement Ratio and Concrete Strength on Flexural Behavior of Concrete Beams. *Journal of Composites for Construction*, V. 2, No. 1 (February): pp. 7–15.

9. Kato, T., and N. Hayashida. 1993. Flexural Characteristics of Prestressed Concrete Beams with CFRP Tendons. In *SP-138: Fiber-Reinforced-Plastic Reinforcement for Concrete Structures—International Symposium*. Farmington Hills, MI: ACI.

10. Maissen, A., and C. M. De Semet. 1995. Comparison of Concrete Beams Prestressed with Carbon Fiber-Reinforced Plastic and Steel Strands. In *Non-Metallic (FRP) Reinforcement for Concrete Structures: Proceedings of the Second International RILEM Symposium (FRPRCS-2)*, ed. L. Taerwe, pp. 430–439. Ghent, Belgium: E & FN SPON.

11. Grace, N. F., and G. A. Sayed. 1997. Behavior of Externally/Internally Prestressed Composite Bridge System. In *Proceedings of the Third International Symposium on Non-Metallic (FRP) Reinforcement for Concrete Structures*, V. 2, pp. 671–678. Sapporo, Japan.

12. Ng, C. K. 2003. Tendon Stress and Flexural Strength of Externally Prestressed Beams. *ACI Structural Journal,* V. 100, No. 5 (September–October): pp. 644–653.

13. Naaman, A. E., and F. M. Alkhairi. 1991. Stress at Ultimate in Unbonded Post-Tensioning Tendons: Part 2—Proposed Methodology. *ACI Structural Journal*, V. 88, No. 6 (November–December): pp. 683–692.

14. Naaman, A. E., and S. M. Jeong. 1995. Structural Ductility of Concrete Beams Prestressed with FRP Tendons. In *Non-Metallic (FRP) Reinforcement for Concrete Structures: Proceedings of the Second International RILEM Symposium (FRPRCS-2)*, ed. L. Taerwe, pp. 379–386. Ghent, Belgium: E & FN SPON.

15. Grace, N. F., T. Enomoto, G. Abdel-Sayed, K. Yagi, and L. Collavino. 2003. Experimental Study and Analysis of a Full-Scale CFRP/CFCC Double-Tee Bridge Beam. *PCI Journal,* V. 48, No. 4 (July–August): pp. 120–139.

16. Grace, N. F. 2000. Response of Continuous CFRP Prestressed Concrete Bridges under Static and Repeated Loadings. *PCI Journal,* V. 45, No. 6 (November–December): pp. 84–102.

17. Taniguchi, H., H. Mutsuyoshi, T. Kita, and A. Machida. 1997. Flexural Behavior of Externally Prestressed Concrete Beams Using CFRP and Aramid Rope under Static and Dynamic Loading. In *Proceedings of the Third International Symposium on Non-Metallic (FRP) Reinforcement for Concrete Structures*, V. 2, pp. 783–790. Sapporo, Japan.

18. Iwamoto, K., Y. Uchita, N. Takagi, and T. Kojima. 1993. Flexural Fatigue Behavior of Prestressed Concrete Beams Using Aramid-Fiber Tendons. In *SP-138: Fiber-Reinforced-Plastic Reinforcement for Concrete Structures—International Symposium*. Farmington Hills, MI: ACI.

19. Grace, N. F., and S. B. Singh. 2003. Design Approach for Carbon Fiber-Reinforced Polymer Prestressed Concrete Bridge Beams. *ACI Structural Journal*, V. 100, No. 3 (May–June): pp. 365–376.

20. Orozco, A. L., and A. K. Maji. 2004. Energy Release in Fiber-Reinforced Plastic Reinforced Concrete Beams. *Journal of Composites for Construction*, V. 8, No. 1 (January): pp. 52–58.

21. Grace, N. F., and G. Abdel-Sayed. 1998. Ductility of Prestressed Concrete Bridges Using CFRP Strands. *Concrete International*, V. 20, No. 6: pp. 25–30.

22. Grace, N. F. 2000. Transfer Length of CFRP/CFCC Strands for Double-T Girders. *PCI Journal*, V. 45, No. 5 (September–October): pp. 110–126.

23. ACI 318. 2002. *Building Code Requirements for Structural Concrete (ACI 318-02) and Commentary (318R-02).* Farmington Hills, MI: ACI.

24. Zou, P. X. W. 2003. Long-Term Properties and Transfer Length of Fiber-Reinforced Polymers. *Journal of Composites for Construction*, V. 7, No. 1: pp. 10–19.

Notation

d = standard diameter

d_b = nominal diameter of strand

$E_{inelastic}$ = inelastic energy absorbed by each bridge model

$E_{inelastic(additional)}$ = additional inelastic energy absorbed by the bridge model after the ultimate load

E_{total} = total energy absorbed by each bridge model

f_c' = compressive strength of concrete

f_{ci}' = compressive strength of concrete at prestress transfer

f_{pi} = amount of prestress in strand at transfer

L_t = transfer length

α_t = 2.12

= transfer length coefficient for carbon-fiber-composite cable strands

ρ = reinforcement ratio

About the authors

Nabil Grace, PhD, P.E., is a University Distinguished Professor and chairman for the Civil Engineering Department and director for the Center for Innovative Materials Research at Lawrence Technological University in Southfield, Mich.

Tsuyoshi Enomoto is an engineer for the Carbon Fiber Cable Department in the New Business Development division of Tokyo Rope Manufacturing Co. Ltd. in Tokyo, Japan.

Ahmed Abdel-Mohti is a graduate student in the Civil Engineering Department at Lawrence Technological University in Southfield, Mich.

Yahia Tokal is a graduate student in the Civil Engineering Department at Lawrence Technological University in Southfield, Mich.

Sreejith Puravankara is a graduate student in the Civil Engineering Department at Lawrence Technological University in Southfield, Mich.

Synopsis

A common problem in prestressed concrete box-beam bridges is the corrosion of steel reinforcement due to seepage of moisture and chemicals through longitudinal cracks in the deck slab between adjacent beams. Replacing conventional steel reinforcement with noncorroding fiber-reinforced-polymer (FRP) reinforcement eliminates the corrosion potential in the concrete member. This paper presents the flexural behavior of box-beam bridge systems that are reinforced with prestressed carbon-fiber-composite cables.

Three box-beam bridge models were designed, constructed, instrumented, and tested to failure. The three bridge models had the same cross section and dimensions. Each bridge model was formed by aligning two precast, prestressed concrete box beams adjacent to each other, filling the gap between the beams with concrete grout, applying transverse post-tensioning, and casting a common deck slab. Each bridge model was reinforced with 14 bottom pretensioned strands, 14 top nonprestressed strands, and 8 bottom nonprestressed strands.

Two of the bridge models contained 12 unbonded longitudinal strands, which were post-tensioned for only one of the models. The third bridge model did not contain any unbonded longitudinal strands. Generally, the model that included unbonded longitudinal post-tensioning demonstrated improved flexural behavior and minimized deflections.

Keywords

Box beam, bridge, corrosion, fiber-reinforced polymer, FRP, reinforcement.

Review policy

This paper was reviewed in accordance with the Precast/Prestressed Concrete Institute's peer-review process.

Reader comments

Please address any reader comments to *PCI Journal* editor-in-chief Emily Lorenz at elorenz@pci.org or Precast/Prestressed Concrete Institute, c/o *PCI Journal*, 209 W. Jackson Blvd., Suite 500, Chicago, IL 60606.